Frequency-dependent interactions determine outcome of competition between two breast cancer cell lines

Audrey R. Freischel[1,2,*], Mehdi Damaghi [1,*], Jessica J. Cunningham[1,2], Arig Ibrahim-Hashim[1],Robert J. Gillies[1], Robert A. Gatenby[1,2], Joel S. Brown[1,2]

[1] Department of Cancer Physiology, Moffitt Cancer Center, Tampa, FL

[2]Department of Integrated Mathematical Oncology, Moffitt Cancer Center, Tampa, FL

*equal contributions

Correspondence:

Experimental: Mehdi.Damaghi@Moffitt.org

Theoretical: Audrey.Freischel@Moffitt.org

Highlights:

Demonstrate how mixed-culture spheroids must be used to characterize competition between two cancer cell lines.

Competition alters growth dynamics of cancer cells.

Competition growth models can be used to quantify density-independent, density-dependent and frequency-dependent effects on competition.

Competition affects tumor progression and structure, making it key to understanding tumor development and evolution.

ABSTRACT:

Tumors are highly dynamic ecosystems in which diverse cancer cell subpopulations compete for space and resources. These complex, often non-linear interactions govern continuous spatial and temporal changes in the size and phenotypic properties of these subpopulations. Because intra-tumoral blood flow is often chaotic, competition for resources may be a critical selection factor in progression and prognosis. Here, we quantify resource competition using 3D spheroid cultures with MDA-MB-231 and MCF-7 breast cancer cells. We hypothesized that MCF-7 cells, which primarily rely on efficient aerobic glucose metabolism, would dominate the population under normal pH and low glucose conditions; and MDA-MB-231 cells, which exhibit high levels of glycolytic metabolism, would dominate under low pH and high glucose conditions. In spheroids with single populations, MCF-7 cells exhibited equal or superior intrinsic growth rates (density-independent measure of success) and carrying capacities (density-dependent measure of success) when compared to MDA-MB-231 cells under all pH and nutrient conditions. Despite these advantages, when grown together, MCF-7 cells do not always outcompete MDA-MB-231 cells. MDA-MB-231 cells outcompete MCF-7 cells in low glucose conditions and coexistence is achieved in low pH conditions. Under all conditions, MDA-MB-231 has a stronger competitive effect (frequency-dependent interaction) on MCF-7 cells than vice-versa. This, and the inability of growth rate or carrying capacity when grown individually to predict the outcome of competition, suggests a reliance on frequency-dependent interactions and the need for competition assays. We frame these results in a game-theoretic (frequency-dependent) model of cancer cell interactions and conclude that competition assays can demonstrate critical density-independent, density-dependent and frequency-dependent interactions that likely contribute to *in vivo* outcomes.

Key Words: cancer cell competition, tumor ecology, tumor evolution, evolutionary therapy

45 **INTRODUCTION:**

46 Each malignant tumor typically contains diverse and heterogeneous habitats due to spatial and temporal
47 variations in cell density, immune infiltration, and blood flow (1-3). Here, we investigate the evolutionary
48 effects of variations in substrate (e.g. glucose, oxygen, and glutamine) and metabolites (e.g. H^+) that are
49 typically governed by alterations in blood flow. These changes, in turn, can alter the local fitness
50 (competitive advantage) of the extant cell populations that can have dramatic evolutionary effects on the
51 phenotypic and genotypic properties of the cancer cells.

52 Recently, two general "niche construction" strategies were observed in clinical and pre-clinical cancers (4, 5).
53 The first consists of cancer cells that possess high levels of aerobic glycolysis that generate an acidic
54 environment, which promotes invasion and protects cells from the immune system. These cells are
55 typically invasive and motile. In the second niche construction strategy, cancer cells promote growth by
56 recruiting and promoting blood vessels. This angiogenic phenotype is typically non-invasive and maintains
57 near-normal aerobic metabolism of glucose. These divergent phenotypes can be found within the same
58 tumor (6-9). The invasive "pioneer" phenotype is optimally adapted to survive and thrive at the tumor
59 edge. There it can co-opt normal tissue vasculature as it invades, and its acidic environment provides
60 protection from immune cells at the tumor-host interface. In contrast, the "engineer" cancer cells are well
61 suited to the interior regions of the tumor where their angiogenic phenotype can, with varying degrees of
62 success, provide blood flow necessary to deliver substrate and remove metabolites. When the pioneers
63 and engineers interact, they presumably compete for both space and substrate. However, the specific
64 phenotypic traits that confer maximal fitness under different micro-environmental conditions have not
65 been well established.

66 Competition between two species leads to four possible outcomes: 1) species A outcompetes B, 2) B
67 outcompetes A, 3) A or B outcompetes the other depending upon who establishes first (alternate stable
68 states), or 4) the two species coexist. These population dynamics can be mathematically framed through

69 the Lotka-Volterra equations for inter-specific competition (10, 11). Derived independently by Lotka
70 (1910) and Volterra (1920), the eponymous equations were first tested empirically by Gause (1932) in the,
71 now classic, competition experiments using various species of *Paramecium* and yeast (12, 13). This, and
72 subsequent work on fruit flies, flour beetles, and various natural systems, have confirmed the predictive
73 power of the Lotka-Volterra equations (14, 15). Such assays utilize growth dynamics to elucidate the
74 critical phenotypic properties that determine fitness under different environmental conditions (16).
75 In ecological systems, growth dynamics are divided into three categories: *density dependent* (DD), *density*
76 *independent* (DI), and *frequency dependent* (FD) effects. Density dependent (DD) effects occur when one
77 cancer cell type outcompetes another because it can achieve a higher equilibrium cell density (carrying
78 capacity) under conditions of space or nutrient limitations. *Density independent* (DI) effects include
79 intrinsic growth rate, which measures the capacity of a cell line to grow exponentially under ideal
80 conditions. In cell biology, these (DD and DI) are often used as indicators of cell fitness (17-19). This,
81 however, ignores the FD interactions, which often determine competitive outcomes. Frequency dependent
82 (FD) effects occur when one cell type outcompetes another because its phenotype disproportionately
83 depresses the growth rate of another as a result of more rapid resource uptake, or via direct interference
84 with the other cell type. This game theoretic effect implies that the success of an individual cell is
85 context dependent. It depends not only on the density of other cells around it, but the phenotypes of
86 those cells as well (20-23). Because of this, FD effects and the outcome of competition can only be
87 evaluated using Gause-style competition assays in which mixtures of the two cell types are grown
88 together using different starting frequencies.
89 Here, we utilize Gause-style competition assays to investigate the competitive interaction between
90 engineer and pioneer phenotypes. These strategies will be represented by the well-characterized MDA-
91 MB-231 and MCF-7 cell lines, which are regularly used *in vitro* and *in vivo* as representative of highly
92 glycolytic and invasive, and low glycolytic and non-invasive phenotypes, respectively (24-26). Any number

93 of cancer cell lines would be good candidates for competition assays covering the myriad of potential
94 factors that affect cellular growth and viability.
95 Assays were conducted in 3D spheroid cultures with varying starting frequencies of each cell type. The
96 spheroid system was selected as an *in vitro* intermediate between 2D cell culture, which may reach an
97 equilibrium state through confluence rather than resource competition, and *in vivo* subcutaneous mouse
98 models, which provide less opportunity for replication and frequent monitoring of the two cell populations
99 (27-34). Spheroids were grown in various combinations of pH and glucose concentrations, letting the 3D
100 structure establish natural nutrient and oxygen gradients. Glutamine availability was also varied to test for
101 growth and competition effects due to secondary nutrients.
102 As in the Gause experiments, measures of growth dynamics were used to evaluate competitive ability. DI,
103 DD, and FD effects corresponded to selection for higher growth rates, carrying capacities, and competitive
104 ability, respectively. Carrying capacities (DD) were estimated from monoculture spheroids under varying
105 culture conditions. Initial growth rates (DI) of each cell type were estimated from both mono- and co-
106 cultured spheroids. As FD effects rely on interactions between cell types, their values were estimated using
107 the Lotka-Volterra competition model. In order to remain agnostic to the mode of tumor spheroid growth,
108 our growth model was selected by first fitting monoculture spheroids to four common growth models
109 (exponential, Monod, logistic, and Gompertz), then selecting the model which best approximated the
110 growth of monoculture spheroids in all culture conditions. This model was then expanded to its two-
111 species competition form and used to obtain estimates of competition coefficients for each cell line under
112 eight different nutrient conditions.
113 We expected both cell types to have higher growth rates and carrying capacities at physiological pH (pH
114 7.4) and higher nutrient levels. MCF-7 cells, which predominantly use oxidative phosphorylation for
115 metabolism of glucose, were predicted to be significantly inhibited by low pH, while MDA-MB-231 cells,
116 which exhibit the Warburg phenotype with high levels of aerobic glycolysis, were expected to be more

117 tolerant. Because the glycolytic MDA-MB-231 cells need more glucose to produce energy compared to the
118 oxygen-consuming MCF-7 cells, we expected the former to respond more favorably to increased glucose
119 concentrations than the latter. We also predicted that, based on their metabolic differences, MCF-7 cells
120 would be fitter under conditions of normal pH and low glucose; and vise-versa for the MDA-MB-231 cells.
121 Herein, we test our hypothesis through competition experiments between the MCF-7 and MDA-MB-231
122 cells under varying environmental conditions. We report the outcome of these competition assays as well as
123 the effect of nutrient availability on DD and DI effects and evaluate their ability to indicate competitive
124 outcome. We used fluorescent measurements to approximate cell growth in the spheroid and propose
125 that the logistic growth equation best approximates the growth of both cell types in the majority of culture
126 conditions. We then used Lotka-Volterra competition equations to determine the contribution of
127 population growth rates (DI), maximal population size (DD) and/or competition coefficients (FD) on the
128 outcome of interspecific competition. Lastly, we compared these results to the outcome of competition
129 between MDA-MB-231 and MCF-7 from mixed tumors *in vivo*.
130
131 **RESULTS:**
132 **MDA-MB-231 generally out-compete MCF-7 cells under all pH, glucose and glutamine levels, and**
133 **starting frequencies**
134 Fluorescently labeled MCF-7 (GFP) and MDA-MB-231 (RFP) cells allowed us to non-destructively measure
135 population dynamics within each micro-spheroid. We used this spheroid system to: 1) observe the
136 outcome of competition (mixed culture), 2) compare population growth models (mono-cultures), 3)
137 measure intrinsic growth rates (DI), 4) measure carrying capacities (DD), and 5) determine competition
138 coefficients (FD). In experiments 1 and 2, spheroids started with a plating density of 20,000 and 10,000
139 cells, respectively, with initial conditions of 0%, 20%, 40%, 60%, 80% and 100% MDA-MB-231 cells relative to
140 MCF-7 cells. In experiment 1, additional treatments included neutral (7.4) versus low (6.5) pH and

141 varying levels of glucose (0, 1, 2, 4.5 g/L) (Figure 1B). Experiment 2 had treatments of pH (7.4, 6.5), glucose (0,
142 4.5 g/L), and glutamine positive and starved media (Figure 1C). The ranges of these values encompass
143 both physiologic and extreme tumor conditions. For example, pH ~6.5 and very low levels of glucose have
144 been measured near the necrotic core of the tumor. Conversely, high glucose and physiologic pH are
145 present at the tumor edge and near vasculature, and also reflect standard culture conditions for our cell
146 lines. Both experiments were further subdivided into parts A and B based on culture conditions (Figure
147 1). In experiment 1, microspheres were grown for 670 hours with fluorescence measured every 24-72
148 hours. In experiment 2, microspheres were grown for 550 hours with fluorescence measured every 6-12
149 hours. Growth medium was replaced every 4 days without disturbing the integrity of the microsphere.
150

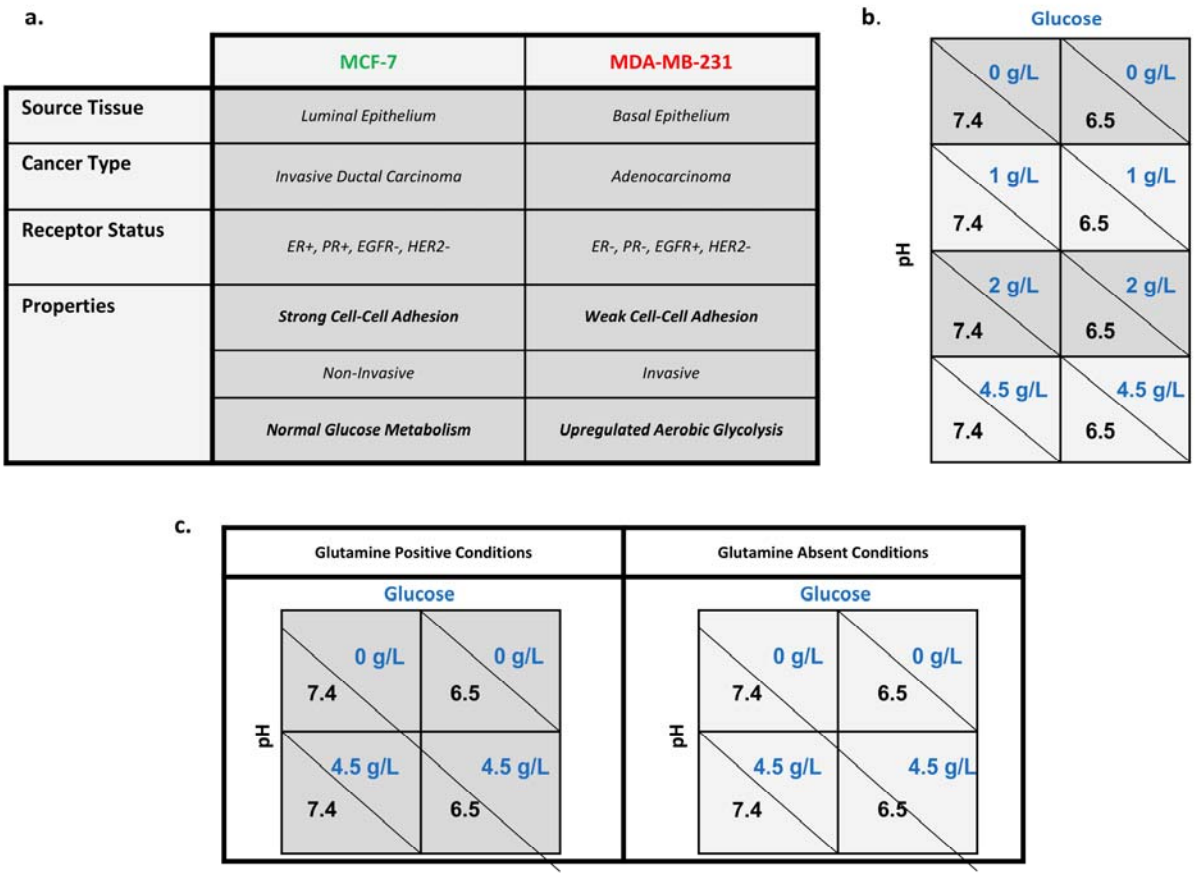

151

152 **Figure 1:** Cell Line Descriptions and Experimental Design A. Phenotype and source information for the

153 “niche constructing” MCF-7 and the “pioneer” MDA-MB-231 cell lines. **B.** Growth dynamics of
154 monoculture and mixed population tumor spheroids in glucose concentrations of 0 g/L and 2 g/L (in
155 dark gray) and of 1 g/L and 4.5 g/L (in light gray) were compared at physiological (7.4) and low (6.5) pH.
156 **C.** Experiment 2 measured the growth dynamics of mixed population tumor spheroids in 4.5 g/L glucose and
157 0 g/L glucose, in physiological (7.4) and low (6.5) pH, and with (in dark gray) and without (in light gray)
158 glutamine to evaluate differences in growth due to the presence of a secondary nutrient.
159
160 Counter to our hypothesis, MDA-MB-231 outcompete MCF-7 cells in physiologic (2 g/L glucose, 7.4 pH)
161 conditions (Figure 2). However, in more acidic conditions (2 g/L glucose, 6.4 pH) the MCF-7 cells appear to
162 persist, suggesting coexistence (Figure 3, Supplementary Figure 1). Furthermore MCF-7 cells persist in
163 either pH condition with high 4 g/L glucose (Figure 4). This raises two questions: 1) Is the success of MDA-
164 MB-231 in most conditions a consequence of higher initial growth rates, increased carrying capacity, or
165 consistently favorable competition coefficients? and, 2) what characteristics of MCF-7 cells allow them to
166 competitively persist at high glucose conditions?
167

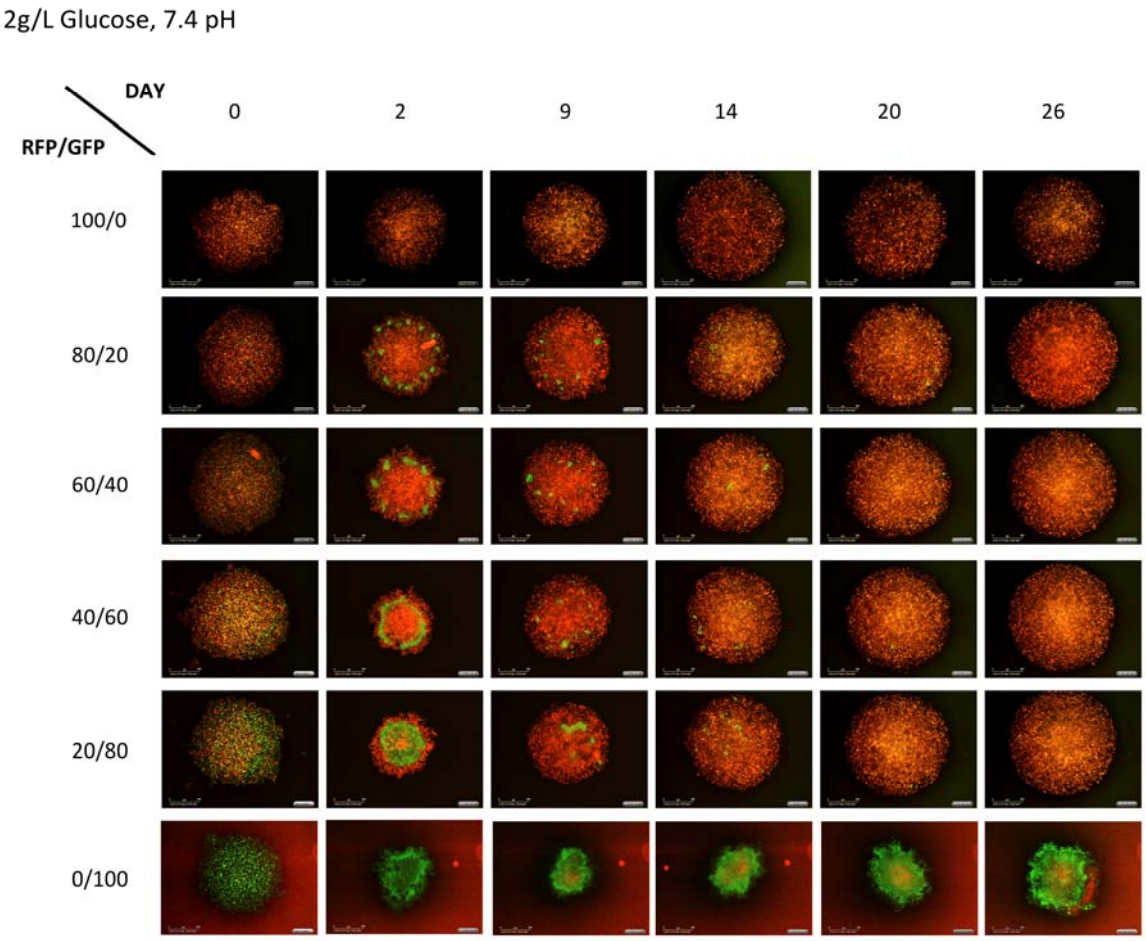

Figure 2: Photographs of spheroids illustrative of the progression and outcome of competition in normal pH. This series shows the progression of spheroids grown physiological conditions (2 g/L glucose, 7.4 pH). Note that, in this case, the MDA-MB-231 cells appear to take over the spheroids by day 20.

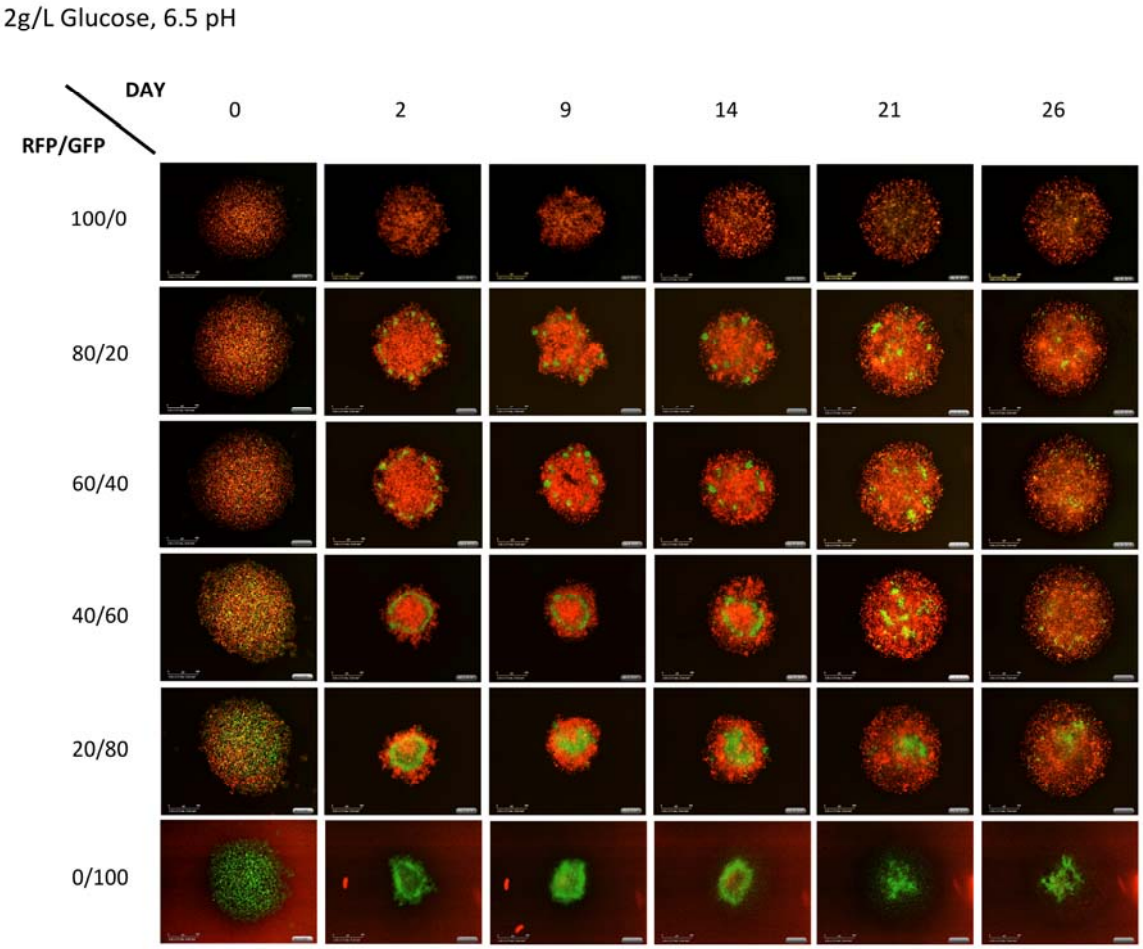

Figure 3: Photographs of spheroids illustrative of the progression and outcome of competition in acidic pH. This series shows the progression of spheroids grown in acidic conditions (6.5 pH) with 2 g/L glucose. Note that, in this case, the MCF-7 cells appear to persist to the end of the experiment.

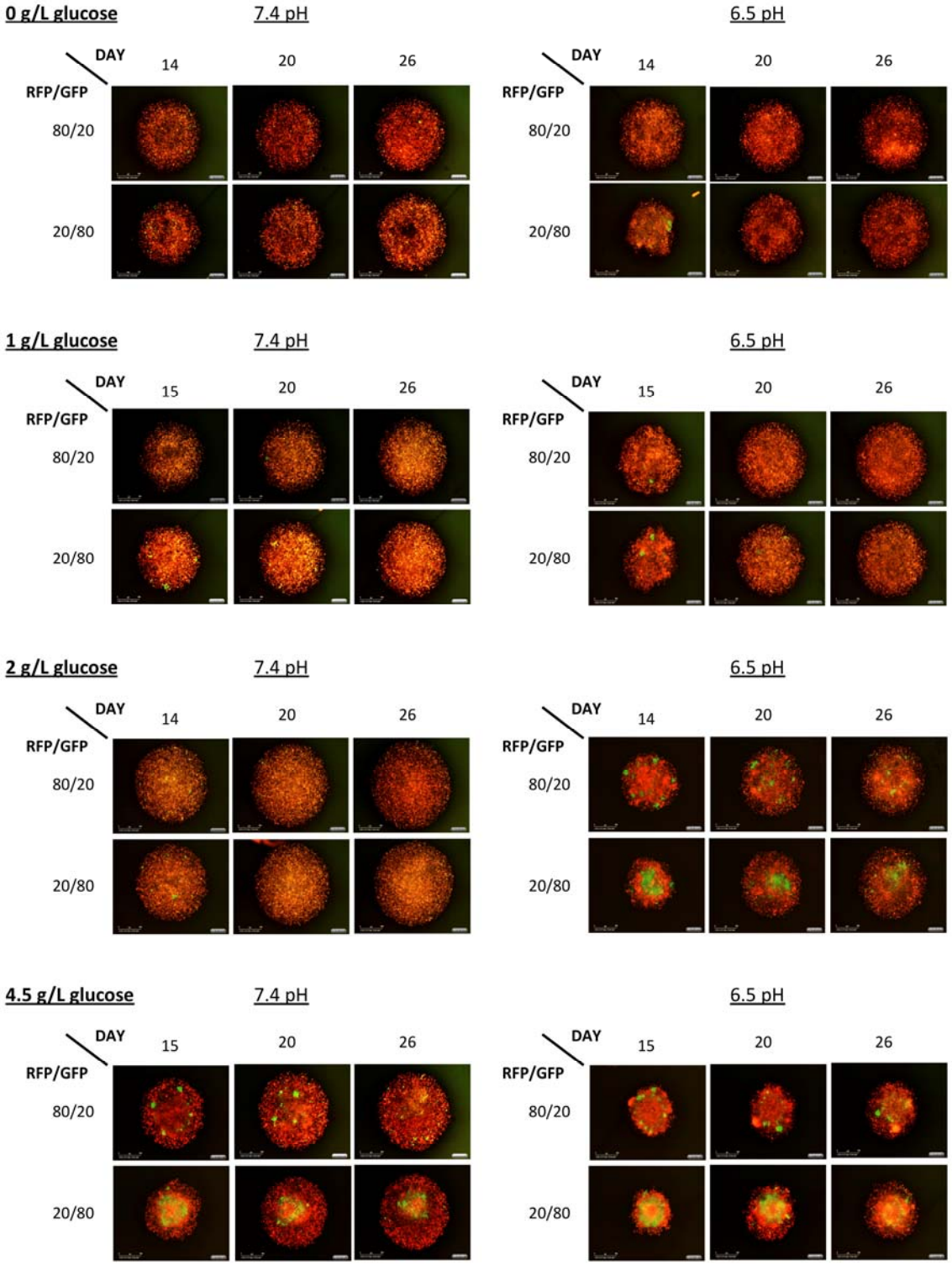

Figure 4: Three time points spanning from the middle to the end for all culture conditions.

181 ***Analysis of Growth Rate***

182 The growth rate of MCF-7 and MDA-MB-231 cells was quantified by measuring the instantaneous
183 exponential growth rate (in units of per day) for each monoculture during the first 72 hours. In general,
184 MCF-7 cells had equal or higher growth rates under all growth conditions when compared to MDA-MB-231
185 cells. MCF-7 cell growth rate was reduced when grown in low pH 6.5 (Figure 5 a-c) environments compared
186 to physiologic pH 7.4 (Figure 5 d-f). Not surprisingly, in the harshest environment of low pH 6.5, no glucose,
187 and no glutamine, MCF-7 cells had the lowest, even negative, growth rate (Figure 5c). Interestingly, the
188 absence of glutamine (Figure5 c and f) reduced the difference in growth rates between the two cell types,
189 regardless of pH or glucose concentration, consistent with glutamine's role as a substrate for respiration,
190 which is more pronounced in MCF-7 cells.

191 While the growth rates of MDA-MB-231 cells during these early time points were generally unaffected by
192 changes in environmental conditions, the initial plating density had a significant effect. The higher (20,000
193 initial calls) plating density (Figure 5 a and d) resulted in slower, even negative, growth rates when
194 compared to the lower (10,000 initial cells) plating density. This suggests that these plating densities may
195 be approaching MDA-MB-231's carrying capacities.

196

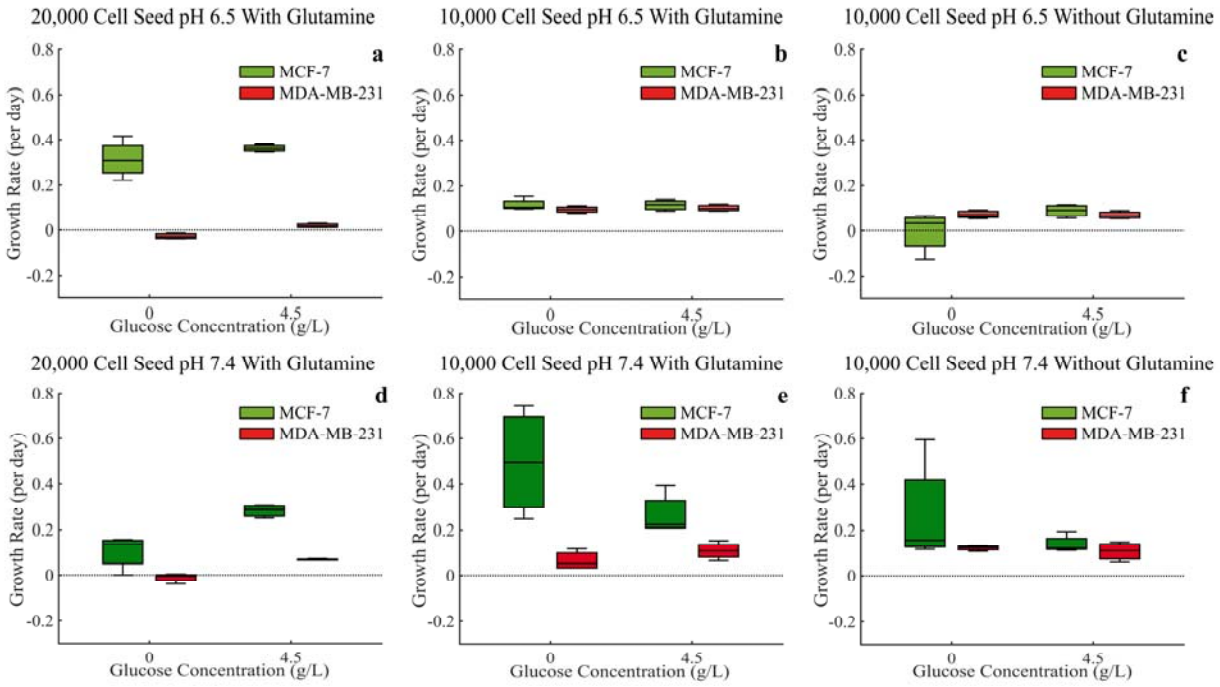

Figure 5: Growth rates of both MCF-7 and MDA-MB-231 cells as measured by the instantaneous exponential growth rate for each monoculture in the first 72 hours under all experimental conditions. ANOVA analysis is provided in Supplemental tables 1-3.

Analysis of Carrying Capacity

Due to some differences in the RFU intensity between the GFP and RFP used for the MCF-7 and MDA-MB-231 cells respectively, a direct comparison of carrying capacity using these RFU measurements cannot be made. In this way we split the results in to two figures (Figure 6 and 7). We see RFU's higher than 60 in the MCF-7 data while the maximum RFU for MDA-MB-231 data is never greater than 20 (please note the varying y-axis limits in the corresponding figures). Even with this difference in RFU intensity, it is not unreasonable to assume, due to the large difference, the MCF-7 cells do indeed have a higher carrying capacity across all experimental conditions.

For MCF-7 cells, an increase in glucose resulted in an increase in carrying capacity across experimental

212 conditions, as would be expected (Figure 6 a-f). Surprisingly, the MCF-7 cells experience a decrease in
213 carrying capacity under normal pH conditions when compared to acidic pH 6.5 conditions suggesting an
214 advantage in acidic conditions.

215

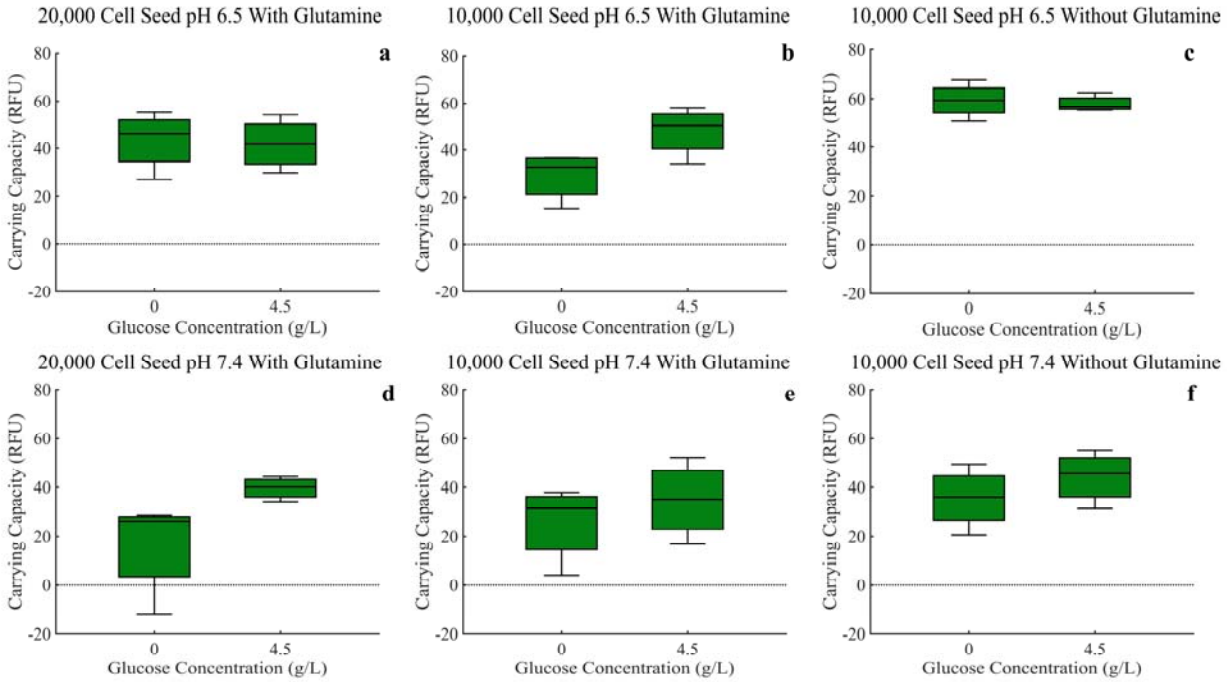

216

217 **Figure 6:** Carrying capacities of MCF-7 cells under all experimental conditions, as measured by the mean
218 fluorescence of the final ten time points. ANOVA analysis is provided in Supplemental tables 4 and 5.

219

220 For the MDA-MB-231 cells, after a high seeding density of 20,000 cells, an increase in glucose resulted in an
221 increase in carrying capacity, just like the MCF-7 cells (Figure 7 a and d). For the low seeding density of
222 10,000 cells, the opposite occurred (Figure 7 b, c, e, and f), though not as dramatically. Furthermore, the
223 MDA-MB-231 cells experience an increase in carrying capacity in normal pH when compared to acidic pH
224 6.5 conditions suggesting an advantage in normal pH conditions.

225

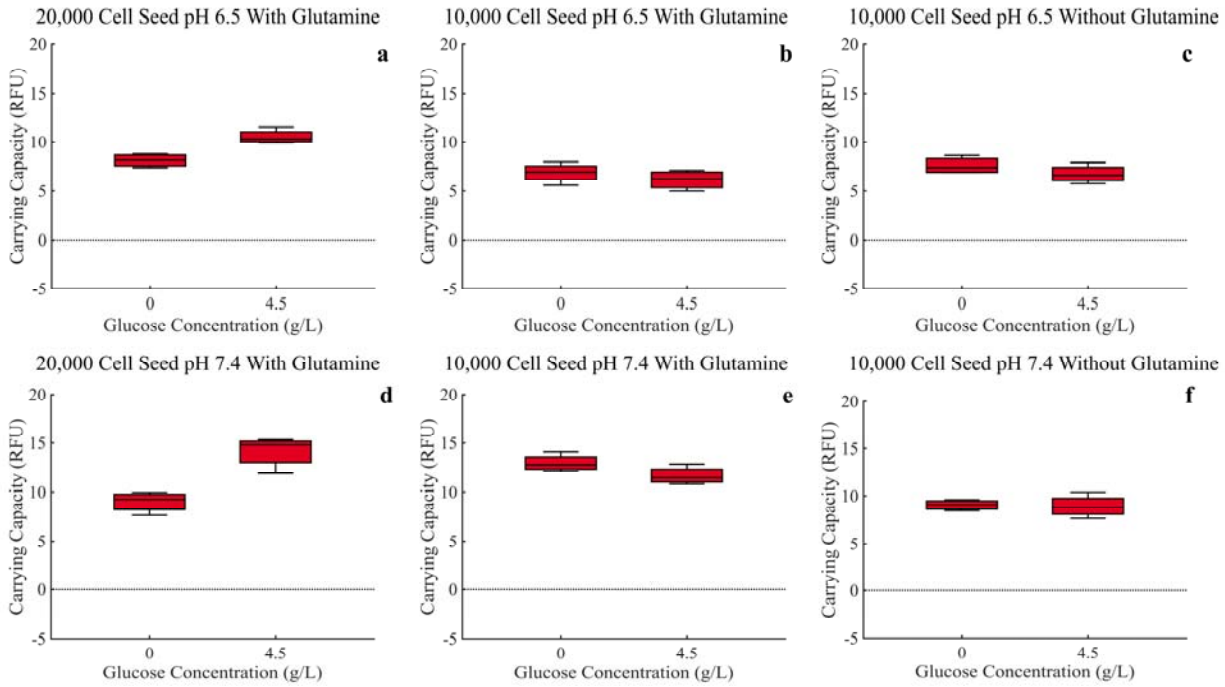

Figure 7: Carrying capacities of MDA-MB-231 cells under all experimental conditions, as measured by the mean fluorescence of the final ten time points. ANOVA analysis is provided in Supplemental tables 4 and 5.

Analysis of Initial Seeding Frequencies

For the analysis of frequency dependent interactions of the two cells lines we analyzed the instantaneous growth rates (in units of per day) during the first 72 hours in the mixed spheroids (Figs. 8 & 9). The figures are split between low glucose conditions of 0 g/L (Fig. 8) and high glucose conditions of 4.5 g/L (Fig. 9). Interestingly, under both glucose environments, MDA-MB-231 cells have their maximum growth rates when there are only a small initial number of MCF-7 cells in the spheroid. This suggests some benefit to the MDA-MB-231 cells from the presence of MCF-7 cells, or less inhibition of growth rates from MCF-7 cells. Furthermore, we see that the MCF-7 cells generally show a maximum growth rate when the seeding frequencies are 40%/60% or 60%/40% (Figure 8 and 9 b, c, e, and f), again suggesting possible benefits to having both cell types in the spheroid.

In low glucose and at the high seeding density of 20,000 cells, the MCF-7 cells experience a significant

241 decrease in growth rate, even negative growth rates, as the seeding frequency of MDA-MB-231 cells
242 increase. This points to the MDA-MB-231 cells potentially approaching the carrying capacity provided
243 within these nutrient starved conditions, essentially fully depleting all the resources for other cell types.
244 When the glucose is increased, these MCF-7 growth rates increase, suggesting there are now sufficient
245 nutrients for both cell types (Figs. 8 and 9 a and d). Upon seeding it appears that both cell types generally
246 have higher initial growth rates when the starting frequencies of MDA-MB-231 are low.
247

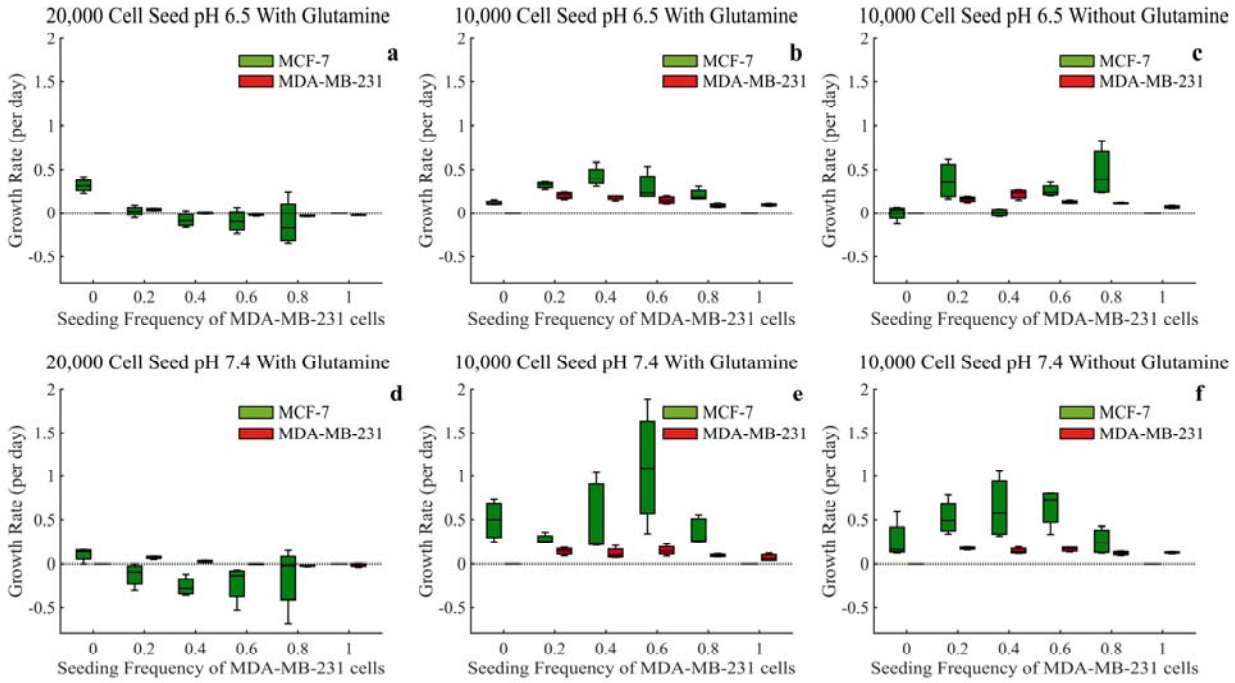

248

249 **Figure 8:** Based on the first 72 hours, estimates of growth rates for mixed population tumor spheroids
250 under glucose starved conditions of 0 g/L. ANOVA analysis is provided in Supplemental tables 1-3.
251

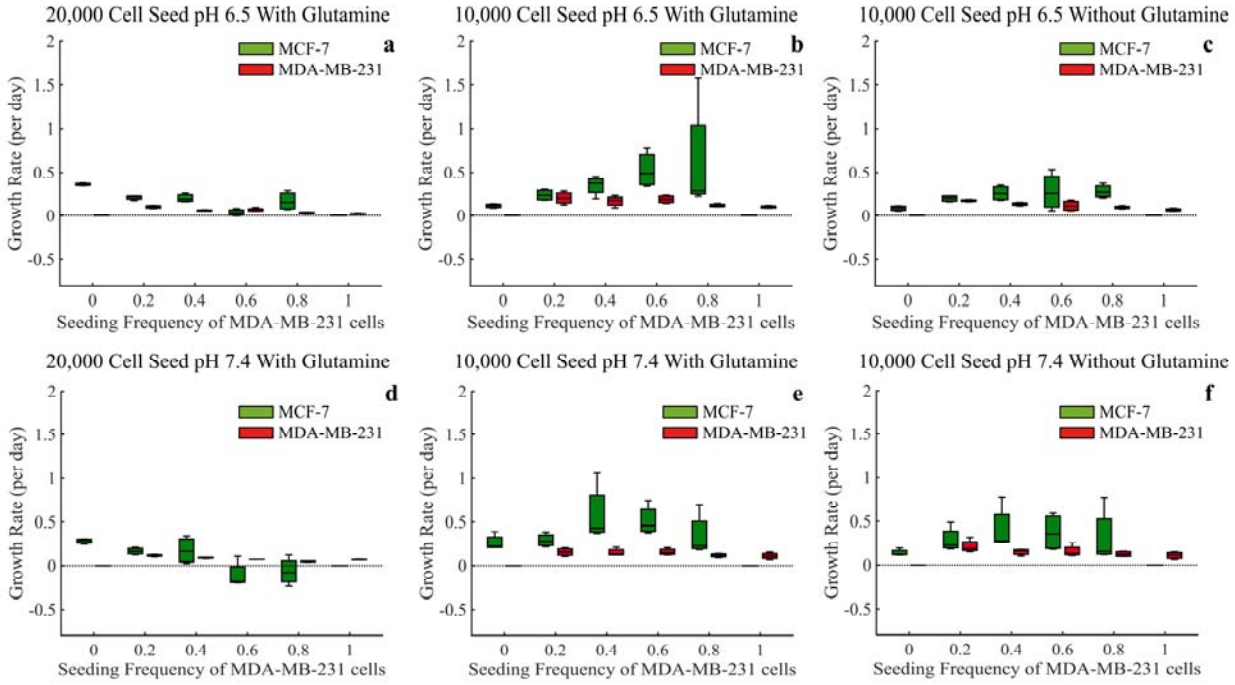

Figure 9: Based on the first 72 hours, estimates of growth rates for mixed population tumor spheroids under glucose rich conditions of 4.5 g/L. ANOVA analysis is provided in Supplemental tables 1-3.

The Logistic Model Best Describes Individual Cell Growth

Frequency-dependent effects (here measured as competition coefficients) can only be quantified by modeling the growth of multiple interacting types or species. In order to obtain an accurate estimate of these, the mode of growth must first be determined. In this way, we use the monoculture spheroids of either MCF-7 or MDA-MB-231 alone as a data set to first understand the growth dynamics without the added complexity of the mixed cultured spheroids. Although several growth models have been proposed for spheroids, tumors, and organoids, no specific consensus has been reached (34, 35). Because of this, we agnostically compared four population growth models: exponential, logistic, Gompertz, and Monod-like (Table 1).

The exponential growth model is commonly used in bacterial studies and assumes unlimited resources. Logistic population growth is the simplest constrained growth model and assumes that per capita

population growth rate declines linearly with population size or density (36). Although it gives a similar shape, Gompertz growth is exponentially constrained by increasing population. Several authors and works have suggested that the Gompertz equation provides a better fit to the growth of tumors in *vivo* (37). The Monod-like equation imagines resource matching where per capita growth rates are proportional to the amount of resources supplied per individual. It provides a good fit to the population growth curves of bacteria and other single cell organisms grown in chemostats (38). Here, we consider all four models when estimating the DI parameter of intrinsic growth rate (r) and the latter three models for estimating the DD parameter of

carrying capacity (K).

Growth Model	Equation	Parameters
Exponential	$\frac{\mathrm{dN}}{\mathrm{dt}} = \mathrm{rN}$	r is instantaneous per capita growth rate
Logistic	$\frac{dN}{dt} = rN\left(1 - \frac{N}{K}\right)$	N is population size
Gompertz	$\frac{dN}{dt} = r\,\mathrm{N} * \ln\left(\frac{K}{N}\right)$	K is the carrying capacity
Monod	$\frac{dN}{dt} = r(K - N)$	

Table 1: The four models considered for estimating the mode of growth of the cancer cells based on data from monoculture spheroids seeded at a low density of 10,000 cells.

Using constrained parameter optimization, all four models were fit to the mono-culture spheroid growth of MCF-7 or MDA-MB-231 cells under the eight environmental conditions (Supplementary Figure 1). Due to the lower number of time points in the experiments with a high seeding density of 20,000 cells, these experiments were not used. Quality of fit for each model was evaluated using adjusted R^2, Root Mean Square Error (RMSE), and Akaike Information Criterion (AIC) (Table 2, Supplementary Table 6).

Model	Cell Line	Measure	4.5 g/L Glucose, 7.4 pH, +Glutamine	4.5 g/L Glucose, 7.4 pH, -Glutamine	4.5 g/L Glucose, 6.5 pH, +Glutamine	4.5 g/L Glucose, 6.5 pH, -Glutamine	0 g/L Glucose, 7.4 pH, +Glutamine	0 g/L Glucose, 7.4 pH, -Glutamine	0 g/L Glucose, 6.5 pH, +Glutamine	0 g/L Glucose, 6.5 pH, -Glutamine
Exponential	MCF-7	Adjusted R^2	0.86375925	0.986878377	0.981146959	0.948234222	0.878382763	0.988394753	0.680927938	0.862338251
		RMSE	4.350169084	1.132653242	1.69847635	3.695432283	3.27179314	1.075082735	2.671205198	8.252546774
		AIC	266.6386	24.91957	97.35169	242.5059	215.3609	15.32116	178.8554	390.336
	MDA-MB-231	Adjusted R^2	0.965940219	0.961195759	0.405939888	0.837579643	0.984098581	0.920137544	0.673358471	0.792081228
		RMSE	0.464566345	0.395146745	0.808032208	0.430099077	0.389104518	0.495043084	0.684053081	0.61219965
		AIC	-135.997	-168.844	-36.3676	-153.248	-167.903	-127.372	-66.3496	-88.2882
Logistic	MCF-7	Adjusted R^2	0.95109814	0.987162238	0.981296804	0.948907945	0.989835743	0.990746769	0.706812568	0.954187534
		RMSE	2.569889623	1.119624296	1.693018458	3.678532642	0.920541516	0.955498916	2.560276438	5.403291938
		AIC	173.8953	24.79074	98.77234	243.6626	-10.9028	-4.37598	173.2207	314.4095
	MDA-MB-231	Adjusted R^2	0.96590504	0.984894861	0.912214515	0.956642704	0.984068806	0.961748527	0.975726308	0.917447748
		RMSE	0.464826241	0.244756935	0.311220709	0.221858188	0.389432857	0.341782758	0.186174247	0.385055441
		AIC	-133.896	-254.978	-206.106	-273.052	-165.751	-193.539	-298.593	-171.604
Monod	MCF-7	Adjusted R^2	0.931940694	0.970120375	0.927134074	0.865196707	0.96774423	0.944005043	0.715360107	0.784133576
		RMSE	3.027431032	1.708127542	3.338320975	5.959270988	1.669117432	2.349660049	2.522459912	11.38349256
		AIC	203.3886	102.5132	220.9842	332.4305	96.2131	161.1858	170.5422	451.5182
	MDA-MB-231	Adjusted R^2	0.942552982	0.987666692	0.874817759	0.962825606	0.939280229	0.972592786	0.965887218	0.921638951
		RMSE	0.603401178	0.221046584	0.370619137	0.205360395	0.759417203	0.288935986	0.220623679	0.375119346
		AIC	-86.9311	-273.726	-174.664	-287.27	-45.5367	-224.445	-268.033	-176.414
Gompertz	MCF-7	Adjusted R^2	0.943527504	0.987314557	0.981080261	0.948061608	0.985336984	0.990179344	0.711173682	0.945493131
		RMSE	2.760461987	1.112887278	1.702046991	3.705015484	1.111112845	0.983955476	2.540994298	5.737193572
		AIC	186.7716	23.68023	99.7297	244.9825	22.96517	1.023868	171.86	325.4425
	MDA-MB-231	Adjusted R^2	0.965812133	0.986346591	0.896293181	0.960341196	0.983941859	0.967290012	0.972497979	0.920364898
		RMSE	0.465418306	0.232605999	0.337719056	0.212122131	0.39072316	0.315765537	0.198161845	0.378158388
		AIC	-133.667	-264.347	-191.397	-281.309	-165.156	-208.107	-287.361	-174.929

Table 2: Average adjusted R^2, RMSE, and AIC when fitting the four growth models to monoculture spheroids.

Two-way ANOVAs (one for each cell type with pH and nutrient levels as independent variables) showed that adjusted R^2's were similar for the three density-dependent models and significantly lower for the exponential model (Supplementary Table 6). Conversely, the RMSE indicated the best fit for exponential growth (lowest value), lowest quality fit for the Monod-like equation, and similar, intermediate values for the logistic and Gompertz growth models. AIC analysis suggests logistic fits to be the best fit in the majority of scenarios.

While any of these four models could be used to model this system, this analysis suggests either an exponential or logistic model provides the best fit to the data. The principal difference between these two

303 models is that logistic growth includes density-dependence and the growth curve approaches a carrying
304 capacity, whereas exponential growth ultimately leads to extinction (if negative growth rates) or infinitely
305 large population sizes (if positive growth rates). In this way, we evaluated whether the spheroids showed
306 evidence of approaching or reaching a carrying capacity. To do this, we examined the slope of the final ten
307 time points for both the red and green fluorescent values (RFU's) for all experimental conditions
308 (Supplementary table 7). As most mono-culture spheroids showed declining slopes, or slopes near to zero,
309 we favor the logistic model for this study.
310
311 ***Parameter Estimation for Lotka-Volterra Competition Model***
312 With the logistic equation showing the best fit for the mono-culture experimental data, we expanded to
313 the Lotka-Volterra competition equations to model the mixed population tumor spheroids. The Lotka-
314 Volterra equations represent a two species extension of logistic growth with the addition of competition
315 coefficients.

$$\frac{dN_1}{dt} = N_1 r_1 \left(1 - \frac{N_1 + \alpha N_2}{K_1}\right)$$

$$\frac{dN_2}{dt} = N_2 r_2 \left(1 - \frac{N_2 + \beta N_1}{K_2}\right)$$

316 where N_i are population sizes, r_i are intrinsic growth rates and K_i are carrying capacities. We let species 1
317 and 2 be MCF-7 and MDA-MB-231, respectively. The competition coefficients (α and β) scale the effects of
318 inter-cell-type competition where α is the effect of MDA-MB-231 on the growth rate of MCF-7 in units of
319 MCF-7, and vice-versa for β. If α (or β) is close to zero, then there is no inter-cell-type suppression; if α or β)
320 is close to 1 then intra-cell-type competition and inter-cell-type competition are comparable; and if α (or β)
321 is >1 then inter-cell-type competition is severe.
322 The values of the carrying capacity of MCF-7 cells K_{MCF}, the carrying capacity of MDA-MB-231 cells K_{MDA},
323 and the competition coefficients, α and β, predict the outcome of inter-specific competition. MCF-7 cells

are expected to outcompete MDA-MB-231 cells if $K_{MCF} > K_{MDA}/\beta$ and $K_{MCF}/\alpha > K_{MDA}$. Similarly, MDA-MB-231 cells are expected to outcompete MCF-7 cells if $K_{MDA}/\beta > K_{MCF}$ and $K_{MDA} > K_{MCF}/\alpha$. Either MCF-7 or MDA-MB-231 will out-compete the other depending upon initial conditions (alternate stable states) when $K_{MCF} > K_{MDA}/\beta$ and $K_{MDA} > K_{MCF}/\alpha$. The stable coexistence of MCF-7 and MDA-MB-231 cells is expected when $K_{MDA}/\beta > K_{MCF}$ and $K_{MCF}/\alpha > K_{MDA}$.

To estimate the values for K_{MCF}, K_{MDA}, α, and β, we fit the co-culture data with low seeding density to the two-species Lotka-Volterra equation creating different fits for each combination of experimental conditions. It is important to note here that the Lotka-Volterra competition equations are not spatially explicit. From Figures 2-4, it can be seen that the cells are segregated within the tumor spheroid. In our application, the Lotka-Volterra competition equations simply provide a first-order linear approximation of between cell-type competition, not a mechanistic model of the consumer-resource dynamics or the spatial dynamics that likely occur in the spheroids.

Using nonlinear constrained optimization, we varied the values for instantaneous growth rates, carrying capacities, and competition coefficients α and β to minimize the RMSE between the Lotka-Volterra model and the experimental data (Figure 10). In addition to estimating the competition coefficients, this uses the mixed culture data to re-estimate the growth rates and carrying capacities previously estimated from the monoculture spheroids as growth rate and carrying capacity depend on initial seeding density (Figs 8-9).

a. **+ Glutamine**

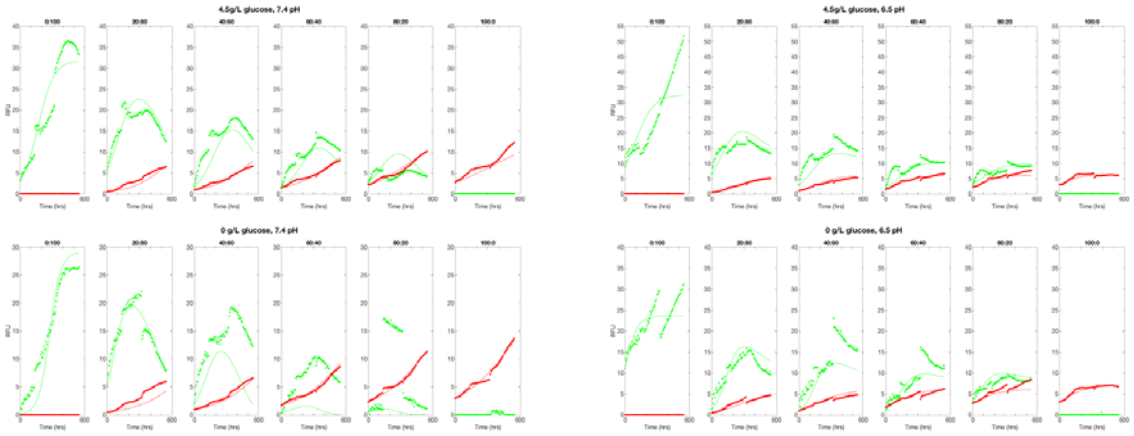

- Glutamine

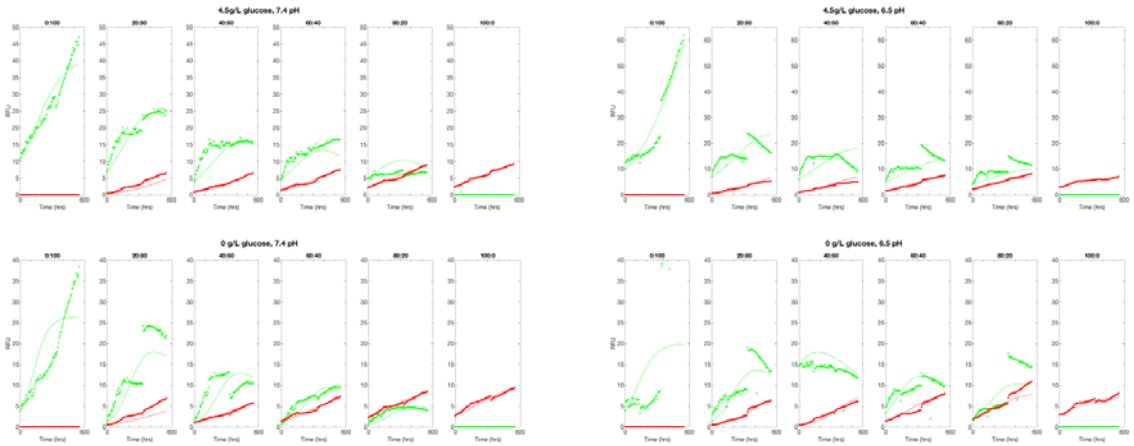

b.

	r_{MCF-7}	$r_{MDA-MB-231}$	K_{MCF-7}	$K_{MDA-MB-231}$	α	β	Outcome
4.5 g/L Glucose, 7.4 pH, +Glutamine	0.013	0.004	31.8	12.9	3.98	-0.243	MDA-MB-231 outcompetes MCF-7
4.5 g/L Glucose, 7.4 pH, -Glutamine	0.008	0.006	40.8	10.4	4.95	0.021	MDA-MB-231 outcompetes MCF-7
4.5 g/L Glucose, 6.5 pH, +Glutamine	0.011	0.010	32.5	6.4	3.69	0.025	Coexistence
4.5 g/L Glucose, 6.5 pH, -Glutamine	0.004	0.006	112.2	6.8	12.64	-0.066	Coexistence
0 g/L Glucose, 7.4 pH, +Glutamine	0.019	0.004	29.2	29.4	7.56	-0.229	MDA-MB-231 outcompetes MCF-7
0 g/L Glucose, 7.4 pH, -Glutamine	0.014	0.006	26.4	10.4	2.90	0.155	MDA-MB-231 outcompetes MCF-7
0 g/L Glucose, 6.5 pH, +Glutamine	0.019	0.009	23.5	7.1	2.51	0.096	Coexistence
0 g/L Glucose, 6.5 pH, -Glutamine	0.012	0.007	20.0	7.4	1.34	-0.080	Coexistence

Figure 10: A. Estimation of growth rates, carrying capacities, and competition coefficients using nonlinear

344 constrained optimization fitting to the Lotka-Volterra competition growth curves to the low (10,000 cell)
345 seeding density experiments. The average of the four replicates for each experimental condition are shown
346 along with the optimized fit to the Lotka-Volterra model. **B.** Optimized parameters for growth rates,
347 carrying capacities, and competition coefficients are shown for each experimental condition. The predicted
348 outcome of competition predicted by these parameters is given in the last column.
349
350 As in the monoculture parameter estimation, MCF-7 had higher intrinsic growth rates and carrying
351 capacities than MDA-MB-231 under all culture conditions. For all culture conditions, $\alpha > 1$ (as high as
352 12.6) and $\beta \approx 0$. This indicates that the MDA-MB-231 cells had large competitive effects on MCF-7
353 growth, and that MCF-7 cells had virtually no inhibitory effects on the growth of MDA-MB-231 cells. It
354 appears that this frequency dependent (FD) effect provides a competitive advantage for the MDA-MB-231
355 cells that allows them to remain in the tumor spheroids despite MCF-7's higher intrinsic growth rates (DI)
356 and carrying capacities (DD).
357 The greatest frequency dependent effect of MDA-MB-231 on MCF-7 (highest α) occurred under conditions
358 of 4.5g/L glucose, 6.5pH, and no glutamine. The greatest effect of MCF-7 cells on MDA-MB-231 (highest β)
359 occurred in the absence of glucose and glutamine at neutral pH. This fits our original predictions; however,
360 the effect of β is not strong enough to rescue MCF-7 cells from competitive exclusion. In accordance with
361 the hypothesis that glucose permits MDA-MB-231 cells to be highly competitive, α's (the effect of MDA-
362 MB-231 on MCF-7) were generally lower under glucose-starved conditions. Further, both cell types appear
363 to experience decreased growth efficiency and competition when glucose/glutamine starved, and under
364 acidic conditions. This is consistent with more general ecological studies showing that competition
365 between species is generally less under harsh physical conditions (39, 40).
366 Using the optimized parameters values calculated by the constrained optimization, analysis of the Lotka-
367 Volterra equations can predict the outcome of competition. This analysis suggests that under physiologic

368 pH, regardless of glucose or glutamine concentration, MDA-MB-231 cells will outcompete the MCF-7 cells.
369 Furthermore, under acidic pH, regardless of glucose or glutamine concentration, MDA-MB-231 cells and
370 MCF-7 cells will actually coexist. This is observed experimentally in Figure 2 and Figure 3 where acidic pH
371 results in coexistence of the two cell types and normal pH results in no MCF-7 cells remaining at the end of
372 the experiment. While a robust result, this does not accord with our original expectations.
373
374 ***In Vivo Exploration of Cell Competition***
375 MDA-MB-231 and MCF-7 cells were grown in the mammary fat pads of 8-10 week old nu/nu female mice.
376 Three tumor models were evaluated: only MCF-7, only MDA-MB-231, and 1:1 mix of both cell types with
377 three replicates for each. Tumor volume was measured weekly. At five weeks, the tumors were
378 harvested and evaluated for ER expression which marks MCF-7 (ER positive) cells providing estimates of
379 the ratio of MDA-MB-231 to MCF-7 cells.
380 H&E staining indicates that MCF-7 tumors had the greatest viability and lowest necrosis while MDA-MB-
381 231 tumors displayed decreased viability and increased necrosis (Figure 11a). The small differences in
382 necrotic and viable tissue between the MDA-MB-231 and mixed tumors are indicative of the expansive
383 effect that MDA-MB-231 phenotype has on tumor progression (Figure 11c).
384 Changes in tumor size over five weeks indicated that MCF-7 cell tumors grew more slowly than MDA-MB-
385 231 tumors and mixed tumors (Figure 11b). This is an interesting result as the in-vitro analysis would have
386 predicted that the MCF-7 tumors would grow the fastest due to both higher growth rate and higher
387 carrying capacity. Only in the harshest in-vitro condition with 0 g/L glucose, acidic pH 6.5, and no glutamine
388 did MCF-7 cells grow more slowly than MDA-MB-231. This potentially suggests that mammary fat pads may
389 exhibit a harsh environment for MCF-7 cells.
390 Of interest, the mixed tumors in-vivo grew significantly faster than the MCF-7 tumors, and potentially
391 faster than the MDA-MB-231 tumors alone beyond 24 days. This reiterates the in-vitro experiments in

392 Figures 8 and 9 where both cell types gain some growth advantage when grown together.

393

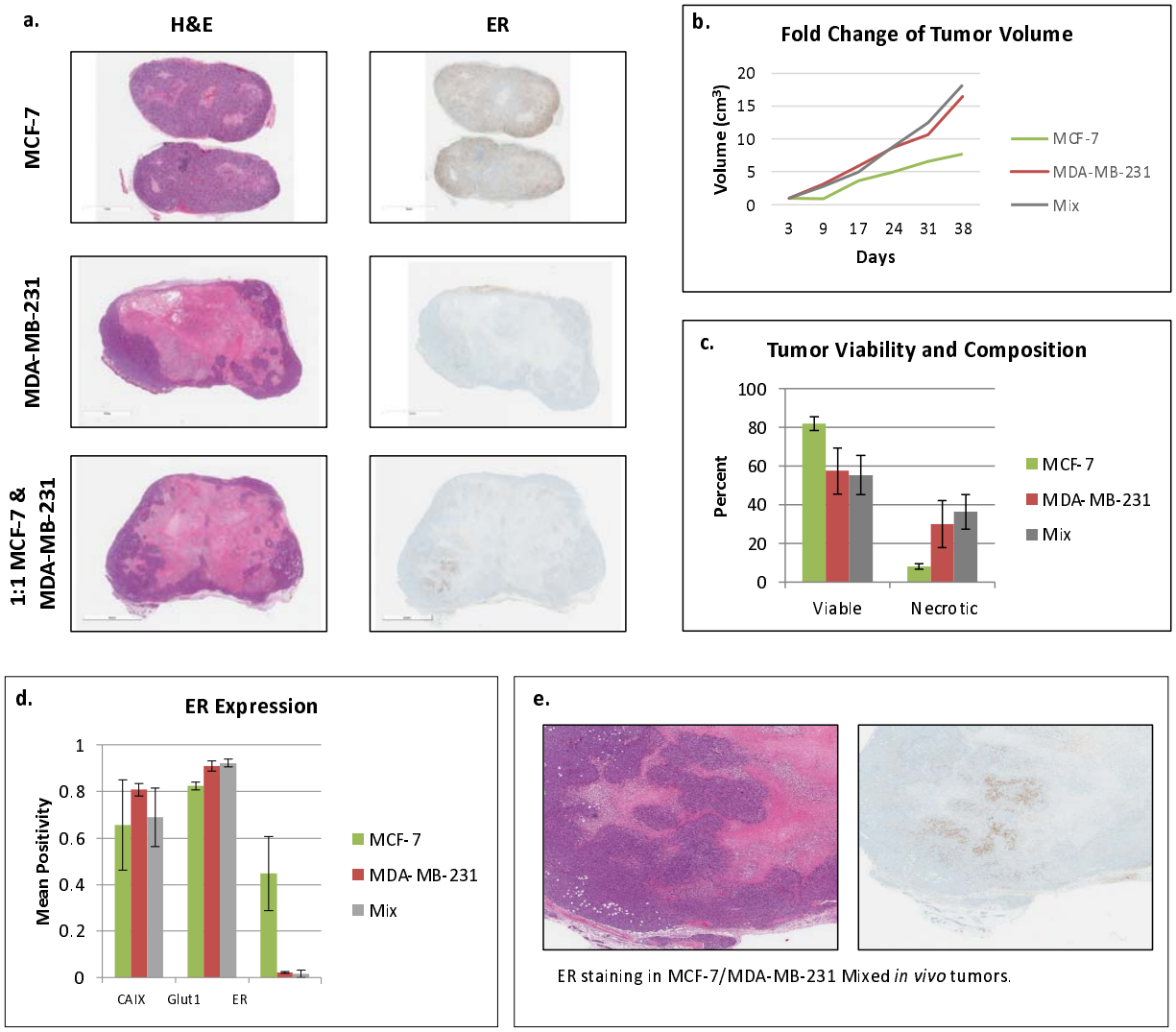

394

395 **Figure 11:** Results of *in vivo* mono- and co- culture tumors. **A.** Histology slides of MCF-7, MDA-MB-231, and
396 1:1 co-cultured tumors. Slides were stained with H&E and ER immune stain. **B.** Average fold change of
397 tumor volume reflects relative growth. **C.** Tumor viability for all three tumor types. Notice a decrease in
398 viability and increase in necrosis in the MDA-MB-231 and mixed tumors. **D.** Measures of CAIX, Glut1, and ER
399 biomarker staining for each tumor type. **E.** The presence of small clumps of ER staining in mixed tumors
400 reflect the clumping of MCF-7 cells in the progression of the mixed tumor spheroids, suggesting the

401 coexistence of these two phenotypes in certain tumor microenvironments.

402

403 Biomarker staining indicated the presence of microenvironment regulating membrane transporters.
404 Variation in CAIX expression between the three tumor types suggests little difference in active pH
405 regulation. Glut1 expression is higher in MDA-MB-231 containing tumors, reflecting the increased capacity
406 for glucose uptake by these cells.

407 ER staining was also used to identify the final frequency of MDA-MB-231 and MCF-7 cells. The amount of
408 ER staining in the mixed tumors (mean of 0.0207) was comparable to the amount found in the MDA-MB-
409 231 only tumor (mean of 0.0227), indicating significant loss of MCF-7 clones at the experiment's end point.
410 This reiterates the results from the in-vitro spheroid experiments demonstrating that MDA-MB-231 cells
411 have a competitive advantage. Interestingly, in one of the mixed tumors (Figure 11e), we note the presence
412 of a cluster of ER positive cells concentrated in an area of interior viable cells. From in-vitro and theoretical
413 analysis, we predict that coexistence of these two cells lines is possible under acidic conditions. In the
414 presumably acidic interior of the in-vivo tumor, while the density of the MCF-7 cells is low, coexistence may
415 be occurring. This clumping MCF-7 cells *in vivo* closely matches the mixed culture *in vitro* spheroids. The
416 spatial distributions of the two cell types may be an important component for coexistence.

417

418 **DISCUSSION:**

419 To understand competition among cancer cell phenotypes within a tumor, we hypothesized that direct
420 competition experiments are critical for understanding factors that may promote or inhibit coexistence.
421 Similar to the classic experiments by Gause, we conducted competition experiments between two well-
422 established breast cancer cell lines that exhibit classic phenotypic and in-vivo growth patterns of the 1)
423 "Pioneer" MDA-MB-231 cells, which are highly invasive, non-angiogenic, and glycolytic and the 2)
424 "Engineer" MCF-7 cells which are angiogenic, non-invasive, estrogen dependent and have near normal

425 glucose metabolism.

426 While here we focused specifically on nutrition and pH as factors that affect cellular competition, there are
427 a number of other factors that undoubtedly play a role. For example, hormonally driven cell lines might
428 elucidate the role of systemic and intratumoral hormone levels in competition experiments such as T47D
429 (ER+, PgR+, HER2-) as another "engineer" instead of MCF7. Or interestingly, one could use the mouse
430 breast cancer cell line MMTV-PyMY (ER-, PgR- Her2+/-) as a "pioneer" instead of MDA-MB-231 cells to
431 elucidate the protein-protein interaction between human and mouse cells. In actuality, any number of
432 cancer cell lines would be good candidates for competition assays covering additional factors that might
433 affect cellular growth and viability.

434 Here, our first experiments investigated monocultures in various nutrition and pH conditions likely to be
435 present in some regions of an *in vivo* tumor. In our experimental spheroid model, the growth rate (r) and
436 carrying capacity (K) for MCF-7 cells in monoculture were the same or greater than those of MDA-MB-231
437 cells under all conditions. We expected these advantages would allow the MCF-7 cells to dominate the
438 MDA-MB-231 cells in co-culture, but surprisingly, MDA-MB-231 cells dominated in all experimental
439 conditions. This counterintuitive result was also found in-vivo, where MCF-7 tumors generally grew slower
440 than MDA-MB-231 tumors. This suggested that the density dependent and density independent
441 interactions can not fully explain cell competition.

442 In this way, the frequency dependent interactions become paramount. We found that magnitude of this
443 frequency dependent competitive effect of one cell type on the other is highly dependent on culture
444 conditions. In spheroids, MDA-MB-231 cells displayed their greatest competitive effect in high glucose and
445 low pH culture conditions while MCF-7 cells, although overall less competitive, showed their greatest
446 competitive effect in low glucose and neutral pH culture conditions. This aligns with the “pioneer” and
447 “engineer” phenotypic patterns and suggests that tumor heterogeneity is driven not only by clonal growth
448 efficiency but also by the landscape of the tumor microenvironment. The mechanisms of this competition is

449 unknown, but there are a number factors that could play a role beyond those tested here such as cytokine
450 production, growth and inhibitory signal dynamics, and direct contact-dependent signals to name a few.
451 In general, the outcome of competition appeared to be pH specific with MDA-MB-231 cells dominating in
452 normal pH conditions and MCF-7 and MDA-MB-231 cells coexisting in acidic conditions both in-vitro and in-
453 vivo. This is evident not only in the overall growth dynamics of competition between MCF-7 and MDA-MB-
454 231 cells, but also by the spatial patterns observed both *in vitro* and *in vivo*. The emergence of such spatial
455 patterns suggests that some aspects of intratumoral spatial distribution are the result of cellular
456 phenotypic properties. In the co-culture spheroids and in the example shown in-vivo, MCF-7 cells form a
457 ring or cluster of highly clumped cells away from the spheroids edge. The MDA-MB-231 cells, on the other
458 hand, formed the spheroid or tumor edge by extending their range outward beyond that of the MCF-7
459 cells. This same pattern, where cells on the periphery of a tumor leave an open niche for another cell type
460 in the interior, has been shown experimentally and also analyzed using Lotka-Volterra competition
461 equations in the *Drosophila* imaginal disc (41-43).
462 The competitive superiority of MDA-MB-231 over MCF-7 from our in vitro and in vivo experiments
463 suggests new hypotheses. Several eco-evolutionary mechanisms may be responsible. In the competition
464 experiments, the cancer cells experienced pulsed resource renewal every 3-4 days. Thus, over a four day
465 period the culture media likely went from nutrient rich to poor, while metabolite concentrations, including
466 acid, increased (44). In both natural and malignant ecosystems, oscillating resources and metabolites
467 favor traits of 1) "priority", 2) speed, and 3) efficiency (45-47).
468 Here, *priority* is defined by the ability to localize, move to, and invade areas of high resource availability.
469 The higher motility and invasiveness of the MDA-MB-231 allowed them to occupy the outer margins of
470 the spheroid where nutrient concentrations would be highest (48). *Speed* is defined by the rate at which an
471 organism can forage. A high speed allows an organism to pre-empt other organisms via interference
472 with uptake by competitors (49). The high glycolytic capacity of the MDA-MB-231 permits them to acquire

473 glucose faster than their MCF-7 competitors on a per cell basis. Furthermore, MDA-MB-231 do not adhere
474 to each other as the MCF-7 cells did. This gives the MDA-MB-231 a higher surface area for nutrient uptake
475 and less cell-to-cell interference in nutrient uptake. Finally, the motility and speed of nutrient uptake may
476 both contribute to rapid but inefficient foraging. High speed and efficiency benefit the cell both through
477 acquisition of resources and by making them unavailable to its competitors.
478 However, high motility and speed of nutrient uptake often result in rapid but inefficient foraging. The lower
479 intrinsic growth rates and carrying capacities of MDA-MB-231 are consistent with this. *Efficiency* is the
480 capacity of an organism to cheaply and profitably exploit resources when they are scarce. The MCF-7 may
481 be slower, more efficient foragers thus depleting nutrients following the pulse more slowly but in a manner
482 that allowed for greater per cell survival and proliferation, thus explaining their higher growth rates and
483 carrying capacity when grown in mono-culture (50, 51).
484 The outcome of competition between the two populations were almost entirely frequency dependent as
485 reflected in the highly asymmetric and strong competitive effect of MDA-MB-231 cells on MCF-7 cells. Yet,
486 we saw an important role for MCF-7's higher carrying capacity (density-dependent effects) in promoting
487 coexistence under some circumstances, and the differences in intrinsic growth rates (density-independent
488 effects) likely influenced the transient dynamics within the mixed cultures.
489

490 **CONCLUSIONS**

491 Mixed-culture competition experiments in spheroids can successfully track competitive outcomes between
492 cell lines of interest (52-54). Because alterations in glucose and pH can significantly affect the competitive
493 ability of different cell phenotypes, manipulation of the microenvironment via therapies could directly
494 influence intra-tumoral evolution and cell-type composition (55-57). Such experiments in spheroids may be
495 valuable for quantifying the costs of resistance. Experiments could consider competing a resistant cell line
496 against its sensitive parental cell line under conditions of no therapy (sensitive would be expected to

497 outcompete the resistant cell line) and under conditions of therapy (resistant should outcompete the
498 sensitive cell line) (58). As accomplished here, one could determine differences in growth rates, carrying
499 capacities and competition coefficients. These metrics would be valuable for informing adaptive therapy
500 trials that modulate therapy so as to maintain a population of sensitive cells as a means for competitively
501 suppressing the resistant cells (59-61).

502 Mixed culture competition experiments demonstrate how both the densities and the frequencies of cell
503 types influence the growth rates and population dynamics of cancer cells. Measurements of resource
504 availability and carrying capacities determine limits to growth. The extent to which inter-specific
505 competition coefficients differ significantly from 1, reveal the extent to which cancer cells engage in eco-
506 evolutionary games where the success of a given cancer cell depends both on its phenotype but the
507 phenotypes of the other cancer cells. Such understanding of how cancer cell types respond to each other
508 and to therapy will be crucial to evolutionarily informed therapies that aim to anticipate and steer the
509 cancer's eco-evolutionary dynamics.

510 **METHODS:**

511 ***Cell Culture and acid adaptation in vitro***

512 MCF-7 and MDA-MB-231 cells were acquired from American Type Culture Collection (ATCC, Manassas,
513 VA, 2007–2010) and were maintained in DMEM-F12, no glutamine, no glucose, no HEPES (Life
514 Technologies) supplemented with 10% FBS (HyClone Laboratories). Cells were tested for mycoplasma
515 contamination and authenticated using short tandem repeat (STR) DNA typing according to ATCC
516 guidelines that is approved by Moffitt Cancer Center. Growth media was supplemented to contain adjusted
517 glucose and glutamine concentrations, depending on desired environmental conditions. Media was also
518 supplemented with 25 mmol/L each of PIPES and HEPES to increase the buffering capacity of the media
519 and the pH adjusted to 7.4 or 6.5 for each spheroid growth condition.

520

521 ***Transfection (GFP/RFP plasmids)***

522 To establish stable cell lines, the MCF-7 and MDA-MB-231 cells were infected with Plasmids expressing
523 RFP or GFP using Fugene 6 (Promega) at an early passage and were selected using 2 µg/ml puromycin
524 (Sigma).

525

526 ***3D spheroid co-culture***

527 Perfecta3 96-Well Hanging Drop Plates or non-adhesive U shape bottom 96 well plates were used to grow the
528 primary spheres containing 10,000 or 20,000 total cells. For each experimental condition, the ratio
529 between MCF-7-GFP and MDA-MB-231-RFP was from 0 to 100 percent as follows: 0/100, 20/80, 40/60,
530 60/40, 80/20, 100/0. Each ratio had four replicates for each experiment. An Incucyte microscope kept at
531 37°C and 5% CO2 was used to image the spheroid growth over approximately 30 days. Images and
532 fluorescent intensity were analyzed in Incucyte built-in software and ImageJ (62). Relative fluorescent
533 units (RFUs) were normalized by averaging red/green fluorescence when the corresponding cell type was

534 absent then subtracting this value from other fluorescent values of that cell type.

535

536 ***Experimental conditions:***

537 Two experiments were conducted. The first consisted of spheroids with a starting density of 20,000 cells
538 under conditions of high (4.5g/L), medium (2g/L), intermediate (1g/L) and no glucose fully crossed with
539 physiological (7.4) and low (6.5) pH. Spheroids were allowed to grow for roughly 670 hours with
540 fluorescence measured every 24-72 hours. Relative fluorescent units (RFUs) were used to generate
541 estimates of growth rates and carrying capacities.

542 Observations from these spheroids prompted us to conduct a second set of experiments consisting of
543 spheroids with a lower starting density (10,000 cells) cultured under the extremes of nutrient
544 concentration (0 g/L and 4.5 g/L glucose) fully crossed with physiological and low pH. Resilience of growth
545 under no glucose prompted a repeat of the experiment 0 g/L and 4.5 g/L glucose fully crossed with
546 physiological and low pH with medium lacking glutamine. To improve accuracy of model-fitting,
547 fluorescent values were collected every 6 or 12 hours.

548

549 **Calculation of growth rate and carrying capacity of mono-cultures:**

550 Growth rates were calculated as the log change of the first 72 hours after plating. Carrying capacities were
551 calculated as the mean fluorescence of the final ten time points for each experiment. Since their values were
552 similar regardless of starting frequency, and since they dominated the tumor spheroid in all experiments, we
553 could estimate the carrying capacities of MDA-MB-231 cells using all cultures with a starting frequency of $\geq$
554 20% MDA-MB-231. Due to competitive effects, MCF-7 carrying capacities were estimated using only the
555 100% MCF-7 spheroids.

556

557 ***Testing among growth models:***

558 Nonlinear constrained optimization was used for parameter estimation of r and K to identify the best fit of

559 the monoculture experiments. The objective function minimized the RMSE between the theoretical curves
560 for exponential, Monod-like, logistic, and Gompertz growth models to the growth dynamics of each
561 monoculture spheroids growth dynamics.
562
563 ***Competition Coefficient Estimation:***
564 Nonlinear constrained optimization was used for parameter estimation of the two-species competition
565 Lotka-Volterra equations. The objective function minimized the cumulative RMSE of all initial seeding
566 densities in order to obtain the parameters that could best explain all experimental initial conditions. For
567 these estimations we allowed the optimization technique to optimize all four parameters: r, K, α, and β.
568 While we could have fixed the growth rates and carrying capacities using the values found during the
569 growth model analysis, we instead allowed them to also vary due to the experimental evidence showing
570 that initial seeding frequency can significantly change the growth rates and carrying capacities of these
571 cells.
572
573 ***In Vivo Tumor Culture:***
574 MCF7 and MDA-MB-231 breast cancer cell lines were purchased from ATCC. Both cells were authenticated by
575 short tandem repeat analysis and tested for mycoplasma. Xenograft studies were performed by the
576 guidelines of the IACUC of the H. Lee Moffitt Cancer Center (that was approved by University of South
577 Florida IACUC committee) using eight- to ten-week-old female nu/nu mice (Envigo). Mice had free access to
578 water and food for the whole duration of the experiment. For MDA-MB-231 and MCF7 mono-tumor
579 formation, 10 million cells were injected into cleared mammary fat pads as described previously (4). For
580 mixed cultures, a 1:1 mixture of 5 million MDA-MB231 and 5 million MCF7 cells were injected. One week
581 before cell injection, an estrogen pellet (0.72 mg slow-release, Innovative Research of America) was
582 implanted to allow for the growth of ER-positive MCF7 tumors. Five weeks later, tumors were harvested.

583

584

585 **References**

586 1. Gillies RJ, Brown JS, Anderson AR, Gatenby RA. Eco-evolutionary causes and consequences of
587 temporal changes in intratumoural blood flow. Nature Reviews Cancer. 2018;18(9):576-85.

588 2. Galon J, Costes A, Sanchez-Cabo F, Kirilovsky A, Mlecnik B, Lagorce-Pagès C, et al. Type, density, and
589 location of immune cells within human colorectal tumors predict clinical outcome. Science.
590 2006;313(5795):1960-4

591 3. Galon J, Mlecnik B, Bindea G, Angell HK, Berger A, Lagorce C, et al. Towards the introduction of the
592 'Immunoscore'in the classification of malignant tumours. The Journal of pathology. 2014;232(2):199-209.

593 4. Lloyd MC, Cunningham JJ, Bui MM, Gillies RJ, Brown JS, Gatenby RA. Darwinian dynamics of
594 intratumoral heterogeneity: not solely random mutations but also variable environmental selection forces.
595 Cancer research. 2016:canres. 2962.015.

596 5. Ibrahim-Hashim A, Robertson-Tessi M, Enriquez-Navas PM, Damaghi M, Balagurunathan Y,
597 Wojtkowiak JW, et al. Defining cancer subpopulations by adaptive strategies rather than molecular
598 properties provides novel insights into intratumoral evolution. Cancer research. 2017;77(9):2242-54.

599 6. Gerlinger M, Rowan AJ, Horswell S, Larkin J, Endesfelder D, Gronroos E, et al. Intratumor
600 heterogeneity and branched evolution revealed by multiregion sequencing. New England journal of
601 medicine. 2012;366(10):883-92.

602 7. Polyak K. Heterogeneity in breast cancer. The Journal of clinical investigation. 2011;121(10):3786-8.

603 8. Perou CM, Sørlie T, Eisen MB, Van De Rijn M, Jeffrey SS, Rees CA, et al. Molecular portraits of human
604 breast tumours. Nature. 2000;406(6797):747.

605 9. Robinson SP, Jordan VC. The paracrine stimulation of MCF-7 cells by MDA-MB-231 cells: possible
606 role in antiestrogen failure. European Journal of Cancer and Clinical Oncology. 1989;25(3):493-7.

607 10. Lotka AJ. Contribution to the theory of periodic reactions. The Journal of Physical Chemistry.
608 1910;14(3):271-4.
609 11. Volterra V. Variazioni e fluttuazioni del numero d'individui in specie animali conviventi: C. Ferrari;
610 1927.
611 12. Gause G. The struggle for existence, 163 pp. Williams and Wilkins, Baltimore. 1934.
612 13. Gause G, Witt A. Behavior of Mixed Populations and the Problem of Natural Selection. The American
613 Naturalist. 1935;69(725):569-609.
614 14. Barker J, Podger R. Interspecific competition between Drosophila melanogaster and Drosophila
615 simulans: effects of larval density on viability, developmental period and adult body weight. Ecology.
616 1970;51(2):170-89.
617 15. Park T. Experimental studies of interspecies competition II. Temperature, humidity, and competition
618 in two species of Tribolium. Physiological Zoology. 1954;27(3):177-238.
619 16. De Wit C, Van den Bergh J. Competition between herbage plants. Journal of Agricultural Science.
620 1965;13:212-21.
621 17. Kimmerling RJ, Prakadan SM, Gupta AJ, Calistri NL, Stevens MM, Olcum S, et al. Linking single-cell
622 measurements of mass, growth rate, and gene expression. Genome biology. 2018;19(1):207.
623 18. Gerstein AC, Otto SP. Cryptic fitness advantage: diploids invade haploid populations despite lacking
624 any apparent advantage as measured by standard fitness assays. PloS one. 2011;6(12):e26599.
625 19. Hart T, Chandrashekhar M, Aregger M, Steinhart Z, Brown KR, MacLeod G, et al. High-resolution
626 CRISPR screens reveal fitness genes and genotype-specific cancer liabilities. Cell. 2015;163(6):1515-26.
627 20. Gallaher J, Brown J, Anderson ARA. The dynamic tumor ecosystem: how cell turnover and trade-offs
628 affect cancer evolution. bioRxiv. 2018:270900.
629 21. Kaznatcheev A, Peacock J, Basanta D, Marusyk A, Scott JG. Fibroblasts and Alectinib switch the
630 evolutionary games played by non-small cell lung cancer. bioRxiv. 2018:179259.

631 22. De Wit CT. On competition. Pudoc; 1960. Report No.: 0372-6223.

632 23. Rodríguez DJ. A method to study competition dynamics using de Wit replacement series
633 experiments. Oikos. 1997;78(2):411-5.

634 24. Comşa Ş, Cimpean AM, Raica M. The story of MCF-7 breast cancer cell line: 40 years of experience in
635 research. Anticancer research. 2015;35(6):3147-54.

636 25. Welsh J. Animal models for studying prevention and treatment of breast cancer. Animal models for
637 the study of human disease: Elsevier; 2013. p. 997-1018.

638 26. Liu K, Newbury PA, Glicksberg BS, Zeng WZ, Paithankar S, Andrechek ER, et al. Evaluating cell lines as
639 models for metastatic breast cancer through integrative analysis of genomic data. Nature communications.
640 2019;10(1):1-12.

641 27. Holliday DL, Speirs V. Choosing the right cell line for breast cancer research. Breast cancer research.
642 2011;13(4):215.

643 28. Neve RM, Chin K, Fridlyand J, Yeh J, Baehner FL, Fevr T, et al. A collection of breast cancer cell lines
644 for the study of functionally distinct cancer subtypes. Cancer cell. 2006;10(6):515-27.

645 29. Kao J, Salari K, Bocanegra M, Choi Y-L, Girard L, Gandhi J, et al. Molecular profiling of breast cancer
646 cell lines defines relevant tumor models and provides a resource for cancer gene discovery. PloS one.
647 2009;4(7):e6146.

648 30. Horwitz K, Costlow M, McGuire W. MCF-7: a human breast cancer cell line with estrogen, androgen,
649 progesterone, and glucocorticoid receptors. Steroids. 1975;26(6):785-95.

650 31. Levenson AS, Jordan VC. MCF-7: the first hormone-responsive breast cancer cell line. Cancer
651 research. 1997;57(15):3071-8.

652 32. Theodossiou TA, Ali M, Grigalavicius M, Grallert B, Dillard P, Schink KO, et al. Simultaneous defeat of
653 MCF7 and MDA-MB-231 resistances by a hypericin PDT–tamoxifen hybrid therapy. NPJ breast cancer.
654 2019;5(1):1-10.

655 33. Sutherland RM, McCredie JA, Inch WR. Growth of multicell spheroids in tissue culture as a model of
656 nodular carcinomas. Journal of the National Cancer Institute. 1971;46(1):113-20.
657 34. Benzekry S, Lamont C, Beheshti A, Tracz A, Ebos JM, Hlatky L, et al. Classical mathematical models
658 for description and prediction of experimental tumor growth. PLoS computational biology.
659 2014;10(8):e1003800.
660 35. Marušić M, Bajzer Ž, Freyer J, Vuk-Pavlović S. Analysis of growth of multicellular tumour spheroids
661 by mathematical models. Cell proliferation. 1994;27(2):73-94.
662 36. Kucharavy D, De Guio R. Application of logistic growth curve. Procedia engineering. 2015;131:280-
663 90.
664 37. Vaghi C, Rodallec A, Fanciullino R, Ciccolini J, Mochel JP, Mastri M, Poignard C, Ebos JM, Benzekry S.
665 Population modeling of tumor growth curves and the reduced Gompertz model improve prediction of the
666 age of experimental tumors. PLoS computational biology. 2020;16(2):e1007178.
667 38. Monod J. The growth of bacterial cultures. Annual review of microbiology. 1949;3(1):371-94.
668 39. Liancourt P, Callaway RM, Michalet R. Stress tolerance and competitive-response ability determine
669 the outcome of biotic interactions. Ecology. 2005;86(6):1611-8.
670 40. Douda J, Doudová J, Hulík J, Havrdová A, Boublík K. Reduced competition enhances community
671 temporal stability under conditions of increasing environmental stress. Ecology. 2018;99(10):2207-16.
672 41. Igaki, T., Pastor-Pareja, J.C., Aonuma, H., Miura, M. and Xu, T., 2009. Intrinsic tumor suppression and
673 epithelial maintenance by endocytic activation of Eiger/TNF signaling in Drosophila. Developmental cell,
674 16(3), pp.458-465.
675 42. Ballesteros-Arias, L., Saavedra, V. and Morata, G., 2014. Cell competition may function either as
676 tumour-suppressing or as tumour-stimulating factor in Drosophila. Oncogene, 33(35), pp.4377-4384.
677 43. Nishikawa, S., Takamatsu, A., Ohsawa, S. and Igaki, T., 2016. Mathematical model for cell
678 competition: Predator–prey interactions at the interface between two groups of cells in monolayer tissue.

679 Journal of theoretical biology, 404, pp.40-50.

680 44. Michl, Johanna, Kyung Chan Park, and Pawel Swietach. "Evidence-based guidelines for controlling
681 pH in mammalian live-cell culture systems." Communications biology 2, no. 1 (2019): 1-12.

682 45. Amend SR, Gatenby RA, Pienta KJ, Brown JS. Cancer foraging ecology: Diet choice, patch use, and
683 habitat selection of cancer cells. Current Pathobiology Reports. 2018;6(4):209-18.

684 46. Brown JS. Coexistence on a seasonal resource. The American Naturalist. 1989;133(2):168-82.

685 47. Chesson P, Gebauer RL, Schwinning S, Huntly N, Wiegand K, Ernest MS, et al. Resource pulses,
686 species interactions, and diversity maintenance in arid and semi-arid environments. Oecologia.
687 2004;141(2):236-53.

688 48. Wells A, Grahovac J, Wheeler S, Ma B, Lauffenburger D. Targeting tumor cell motility as a strategy
689 against invasion and metastasis. Trends in pharmacological sciences. 2013;34(5):283-9.

690 49. Hagy HM, Kaminski RM. Determination of foraging thresholds and effects of application on energetic
691 carrying capacity for waterfowl. PLoS One. 2015;10(3).

692 50. Richards SA, Nisbet RM, Wilson WG, Possingham HP. Grazers and diggers: exploitation competition
693 and coexistence among foragers with different feeding strategies on a single resource. The American
694 Naturalist. 2000;155(2):266-79.

695 51. Taylor TB, Wass AV, Johnson LJ, Dash P. Resource competition promotes tumour expansion in
696 experimentally evolved cancer. BMC evolutionary biology. 2017;17(1):268.

697 52. Beaupain R. A method for three-dimensional coculture of cancer cells combined to any other type of
698 cells maintained organotypically. Methods in cell science. 1999;21(1):25-30.

699 53. Hirschhaeuser F, Menne H, Dittfeld C, West J, Mueller-Klieser W, Kunz-Schughart LA. Multicellular
700 tumor spheroids: an underestimated tool is catching up again. Journal of biotechnology. 2010;148(1):3-15.

701 54. Weiswald L-B, Bellet D, Dangles-Marie V. Spherical cancer models in tumor biology. Neoplasia.
702 2015;17(1):1-15.

703 55. Sutherland RM. Importance of critical metabolites and cellular interactions in the biology of
704 microregions of tumors. Cancer. 1986;58(8):1668-80.
705 56. Sutherland RM. Cell and environment interactions in tumor microregions: the multicell spheroid
706 model. Science. 1988;240(4849):177-84.
707 57. Mueller-Klieser W, Freyer J, Sutherland R. Influence of glucose and oxygen supply conditions on the
708 oxygenation of multicellular spheroids. British journal of cancer. 1986;53(3):345.
709 58. Tofilon PJ, Arundel CM, Deen DF. Response to BCNU of spheroids grown from mixtures of drug-
710 sensitive and drug-resistant cells. Cancer chemotherapy and pharmacology. 1987;20(2):89-95.
711 59. Gatenby RA, Silva AS, Gillies RJ, Frieden BR. Adaptive therapy. Cancer research. 2009;69(11):4894-
712 903.
713 60. Gallaher JA, Enriquez-Navas PM, Luddy KA, Gatenby RA, Anderson AR. Spatial heterogeneity and
714 evolutionary dynamics modulate time to recurrence in continuous and adaptive cancer therapies. Cancer
715 research. 2018;78(8):2127-39.
716 61. Zhang J, Cunningham JJ, Brown JS, Gatenby RA. Integrating evolutionary dynamics into treatment of
717 metastatic castrate-resistant prostate cancer. Nature communications. 2017;8(1):1816.
718 62. Rasband, W.S., ImageJ, U. S. National Institutes of Health, Bethesda, Maryland, USA,
719 https://imagej.nih.gov/ij/, 1997-2018.
720
721
722

ACKNOWLEDGEMENTS:

We thank Jeffrey West for assistance with software, we thank Chris Whelan and Dorothy Wallace for discussion and good ideas. Funding was provided by NIH/NCI 1U54CA193489-01A1, Cancer as a Complex Adaptive System, NIH/NCI U54 Supplement, The tumor-host evolutionary arms race, and R01 CA077575. This work was supported in part by the Analytic Microscopy Core Facility and the Tissue Core Facility at the H. Lee Moffitt Cancer Center & Research Institute; an NCI designated Comprehensive Cancer Center (P30-CA076292).

AUTHOR CONTRIBUTIONS:

All authors participated in the study ideas and the writing of the paper. M.D., A.I., A.R.F. and J.S.B designed the experiments. M.D., A.I. and A.R.F. collected the data. A.R.F., J.J.C. and J.S.B. performed the statistical analyses.

COMPETING INTERESTS:

The authors declare no competing financial interests.